

# Analysis of the unbound spectrum of $^{12}\text{Li}$

Z. X. Xu<sup>a</sup>, R. J. Liotta<sup>a</sup>, C. Qi<sup>a,\*</sup>, T. Roger<sup>b</sup>, P. Roussel-Chomaz<sup>b</sup>,  
H. Savajols<sup>b</sup>, R. Wyss<sup>a</sup>

<sup>a</sup>*Royal Institute of Technology (KTH), Alba Nova University Center, SE-10691  
Stockholm, Sweden*

<sup>b</sup>*GANIL, CEA/DSM - CNRS/IN2P3, Bd Henri Becquerel, BP 55027, F-14076 Caen  
Cedex 5, France*

---

## Abstract

The unbound nucleus  $^{12}\text{Li}$  is evaluated by studying three-neutron one-proton excitations within the multistep shell model in the complex energy plane. It is found that the ground state of this system consists of an antibound  $2^-$  state. A number of narrow states at low energy are found which ensue from the coupling of resonances in  $^{11}\text{Li}$  to continuum states close to threshold.

*Keywords:* Shell model, Berggren representation,  $^{12}\text{Li}$

---

## 1. Introduction

The study of halo nuclei is one of the main subjects of research in nuclear physics at present. Many theoretical predictions on halo, superhalo and antihalo nuclei have been advanced in recent years [1, 2, 3]. Most of these calculations correspond to nuclei very far from the stability line. They are mainly thought as a guide for experiments to be performed in coming facilities. The general feature found in these calculations is that a necessary condition for a nucleus to develop a halo is that the outmost nucleons move in shells which extend far in space. That is, only a weak barrier keep the system within the nuclear volume. These shells may be resonances, antibound states (also called virtual states), or even low-spin bound states which lie very close to the continuum threshold. These conditions are fulfilled by the nucleus  $^{11}\text{Li}$  and also heavier Li isotopes. There are a number of experiments

---

\*Corresponding author.

*E-mail address:* chongq@kth.se (Chong Qi)

which have been performed in these very unstable isotopes in order to get information about the structure of halos [4]. In particular we will concentrate our attention to Refs. [5, 6, 7] where the spectrum of  $^{12}\text{Li}$  was measured. Our aim is to analyze these experimental data by using a suitable formalism to treat unstable nuclei. This formalism is an extension of the shell model to the complex energy plane and is therefore called complex shell model [8], although the name Gamow shell model is also used [9]. In addition, the correlations induced by the pairing force acting upon particles moving in decaying single-particle states will be taken into account by using the multistep shell model (MSM) [10].

The formalism is presented in Section 2. Applications are in Section 3 and a summary and conclusions are in Section 4.

## 2. The formalism

The study of unstable nuclei is a very difficult undertaking since, in principle, time dependent formalisms should be used to describe the motion of a decaying nucleus. However, the system may be considered stationary if it lives a long time. In this case the time dependence can be circumvented. In fact, often unstable nuclei live a very long time and therefore they may be considered bound as, e.g., in alpha decaying states of many heavy isotopes, like  $^{208}\text{Bi}$  or  $^{180}\text{Ta}(9^-)$ , with  $T_{1/2} > 10^{15}y$ . On the other hand, experimental facilities allow one nowadays to measure systems living a very short time. To describe these short time processes one has to consider the decaying character of the system.

Of the various theories that have been conceived to analyze unbound systems, we will apply an extension of the shell model to the complex energy plane [8]. The basic assumption of this theory is that resonances can be described in terms of states lying in the complex energy plane. The real parts of the corresponding energies are the positions of the resonances while the imaginary parts are minus twice the corresponding widths, as it was proposed by Gamow at the beginning of quantum mechanics [11]. These complex states correspond to solutions of the Schrödinger equation with outgoing boundary conditions. We will not present here the formalism in detail, since this was done many times before, e.g., in Refs. [12, 13]. Rather, we will give the main points necessary for the presentation of the applications.

### 2.1. The Berggren representation

In this Subsection we will very briefly describe the representation to be used here.

The eigenstates of a central potential obtained as outgoing solutions of the Schrödinger equation can be used to express the Dirac  $\delta$ -function as [14],

$$\delta(r - r') = \sum_n w_n(r)w_n(r') + \int_{L^+} dE u(r, E)u(r', E), \quad (1)$$

where the sum runs over all the bound and antibound states plus the complex states (resonances) which lie between the real energy axis and the integration contour  $L^+$ . The wave function of a state  $n$  in these discrete set is  $w_n(r)$  and  $u(r, E)$  is the scattering function at energy  $E$ . The antibound states are virtual states with negative scattering length. They are fundamental to describe nuclei in the Li region [15].

The resonances and the antibound states are poles of the single-particle Green function and, therefore, we will call them "poles" in order to make a distinction with the scattering states. This is important since it is through the poles that we will recognize physically meaningful states, i. e. states that live a time long enough. Although meaningful states are usually immersed among continuum states, they can be recognized because their wave functions contain important contributions from the poles, as will be seen in the Applications.

Discretizing the integral of Eq. (1) one obtains the set of orthonormal vectors  $|\varphi_j\rangle$  forming the Berggren representation [16]. Since this discretization provides an approximate value of the integral, the Berggren vectors fulfill the relation  $I \approx \sum_j |\varphi_j\rangle\langle\varphi_j|$ , where all states, that is bound, antibound, resonances and discretized scattering states, are included. The corresponding single-particle wave functions are

$$\langle\vec{r}|\varphi_i\rangle = R_{n_i l_i j_i}(r)(\chi_{1/2} Y_{l_i}(\hat{r}))_{j_i m_i}, \quad (2)$$

where  $\chi$  is the spin wave function and

$$R_{n_i l_i j_i}(r) = \phi_{n_i l_i j_i}(r)/r \quad (3)$$

is the radial wave function fulfilling the Berggren metric, according to which the scalar product between two functions consists of one function times the other (for details see Ref. [16]), i.e.,

$$\int_0^\infty dr \phi_{n_i l_i j_i}(r) \phi_{n'_i l'_i j'_i}(r) = \delta_{n_i n'_i}. \quad (4)$$

We will apply the Berggren representation to analyze the spectrum of  $^{12}\text{Li}$  by using the Multistep Shell Model Method [10] (MSM). In order to make the presentation clear we will give a short description of the main points to be used in this paper.

The Berggren representation has been used before within the framework of the CXSM (or the Gamow Shell Model, which is the same [13]) to study Li isotopes [17]. The core in these calculations was assumed to be  $^4\text{He}$  and the Shell Model single-particle states were the shells  $0p$  only. As pointed out in that reference, the study of many particles moving in states lying in the complex energy plane can be a challenging task. The main problem is that due to the presence of the scattering states the dimension of the Berggren basis soon becomes very large, as well as non-Hermitian and complex. Therefore in [17] one could describe well light Li isotopes, up to  $^9\text{Li}$ . But in heavier isotopes the state  $1s_{1/2}$  (which is an antibound state) is of a fundamental importance and its inclusion would make the application of the CXSM a prohibitive undertaking [17]. The importance of the antibound state in this nuclear region was known since a rather long time [15]. An excellent explanation of the halo nucleus  $^{11}\text{Li}$  was given in Ref. [18] by using the Continuum Shell Model, including in the representation only the neutron waves  $s_{1/2}$ ,  $p_{1/2}$  and  $d_{3/2}$ , which in terms of the CXSM implies to include the antibound state and the resonances  $0p_{1/2}$  and  $0d_{3/2}$ , but not the state  $0p_{3/2}$ . The corresponding CXSM calculation was indeed performed in Refs. [19, 20] and, perhaps not surprising, one could thus explain well the structure of  $^{11}\text{Li}$  as well as the corresponding halo.

One way of avoiding too large dimensions is by including in the basis only physically meaningful states. These are states which govern the calculated quantities. For instance, in the evaluation of  $^6\text{Li}$  the single-particle resonance  $0p_{1/2}$  is very broad and its inclusion does not affect the results appreciably [17]. In this context, one important point that has to be emphasized is the evolution of the single-particle states in these isotopes as the continuum threshold is reached. In light Li isotopes the unstable character of the unbound states is reflected by the CXSM in that the neutron resonance  $0p_{1/2}$  is very broad and plays practically no role in the evaluation of the spectrum. Instead, starting in  $^9\text{Li}$  this state becomes extremely important and in  $^{11}\text{Li}$  contributes by about 50% to the formation of the halo [20, 21]. On the other hand, the state  $0p_{3/2}$  is fundamental in the structure of light Li isotopes, but its importance is diminished to a point where it can be neglected starting in  $^{10}\text{Li}$ . Shell Model calculations performed within this approximation repro-

duced very well the experimental data [18, 20, 22]. Even three-body (Fadeev) approaches [21, 23] have shown that the structure of heavy Li isotopes are not appreciably affected by the state  $0p_{3/2}$ .

An important conclusion of all the calculations mentioned above is that the low lying states in  $^{11}\text{Li}$  are essentially two-neutron excitations. Moreover, the corresponding single-neutron states, forming the CXSM representation, are in a similar way extracted from the odd-neutron excitations in  $^{10}\text{Li}$  [20, 21]. It is to be noticed that in these references the proton degrees of freedom were also neglected. The reason for this is that the pairing interaction acting upon the even number of neutrons present in odd Li isotopes determines the spectrum, leaving the protons as mere spectators. However, this cannot be said in our case of  $^{12}\text{Li}$ . We will therefore include in the calculations the proton shell  $0p_{3/2}$ .

In our three-neutron one-proton case a way of distinguishing physically meaningful states is by considering first the two-neutron excitations. From the calculated states one can single-out the resonances which are very broad or otherwise unphysical (for instance energy eigenvalues with real as well as imaginary negative parts).

In order to introduce the physically meaningful two-neutron states in the formalism we will apply the MSM. In this method one solves the Shell Model equations in several steps. One first chooses a single-particle representation. Then one evaluates the two-body equations. Next one solves the three-body equations within a basis consisting of the tensorial product of the one- and two-body basis previously evaluated. For the four-particle case one can choose as a basis the one- times three-particle basis states already evaluated or the two- times two-particle basis, and so on. In our case we will first solve the two-neutron states as done in Refs. [20]. We will thus sort out the physical meaningful states to be used in the three-neutron case. Besides the advantage of reducing the basis dimensions, the inclusion of these meaningful two-particle states implies that relevant continuum (scattering) states, that is those continuum states that determine the physically meaningful two-particle resonances, are also included.

In the next MSM step we will evaluate the three-neutron states in a basis consisting of the one- times two-particle states. Finally, with the three-neutron states thus determined we will form the one-proton three-neutron MSM basis to evaluate the spectrum of  $^{12}\text{Li}$ .

The formalism corresponding to these calculations starts by choosing the single-particle (Berggren) states. Using the Berggren representation thus

chosen one gets the two-particle shell-model equations in the complex energy plane (CXSM) [12], i.e.,

$$(W(\alpha_2) - \epsilon_i - \epsilon_j)X(ij; \alpha_2) = \sum_{k \leq l} \langle \tilde{k}\tilde{l}; \alpha_2 | V | ij; \alpha_2 \rangle X(kl; \alpha_2), \quad (5)$$

where  $V$  is the residual interaction. The tilde in the interaction matrix element denotes mirror states so that in the corresponding radial integral there is not any complex conjugate, as required by the Berggren metric. The two-particle states are labeled by  $\alpha_2$  and Latin letters label single-particle states.  $W(\alpha_2)$  is the correlated two-particle energy and  $\epsilon_i$  is single-particle energy. The two-particle wave function is given by

$$|\alpha_2\rangle = P^+(\alpha_2)|0\rangle, \quad (6)$$

where the two-particle creation operator is given by,

$$P^+(\alpha_2) = \sum_{i \leq j} X(ij; \alpha_2) \frac{(c_i^+ c_j^+)_{\lambda_{\alpha_2}}}{\sqrt{1 + \delta_{ij}}}, \quad (7)$$

and  $\lambda_{\alpha_2}$  is the angular momentum of the two-particle state.

We will use a separable interaction, as in Ref. [20], which describes well the two-neutron states in  $^{11}\text{Li}$ . The energies are thus obtained by solving the corresponding dispersion relation. The two-particle wave function amplitudes are given by [20]

$$X(ij; \alpha_2) = N_{\alpha_2} \frac{f(ij, \alpha_2)}{\omega_{\alpha_2} - (\epsilon_i + \epsilon_j)}, \quad (8)$$

where  $f(ij, \alpha_2)$  is the single particle matrix element of the field defining the separable interaction and  $N_{\alpha_2}$  is the normalization constant determined by the condition  $\sum_{i \leq j} X(ij; \alpha_2)^2 = 1$ .

With the two-neutron states thus evaluated we proceed to the calculation of the three-neutron states by using the MSM in the complex energy plane (CXMSM), as briefly described below.

## 2.2. The Multistep Shell Model Method

As its name indicates, the Multistep Shell Model Method (MSM) solves the shell model equations in several steps. In the first step the single-particle representation is chosen. In the second step the energies and wave functions

of the two-particle system are evaluated by using a given two-particle interaction. The three-particle states are evaluated in terms of a basis consisting of the tensorial product of the one- and two-particle states previously obtained. In this step the interaction does not appear explicitly in the formalism. Instead, it is the wave functions and energies of the components of the MSM basis that replace the interaction. The MSM basis is overcomplete and non-orthogonal. To correct this one needs to evaluate the overlap matrix among the basis states. A general description of the formalism is in Ref. [10]. The particular system that is of our interest here, i.e., the three-particle case, can be found in Ref. [24], where the MSM was applied to study the three-neutron hole states in the nucleus  $^{205}\text{Pb}$ .

Using the Berggren single-particle representation described above, we will evaluate the complex energies and wave functions of  $^{12}\text{Li}$  using the MSM basis states consisting of the Berggren one-particle states, which are states in  $^{10}\text{Li}$ , times the two-neutron excitations that determine the low lying spectrum of  $^{11}\text{Li}$ . Below we refer to this formalism as CXMSM.

The three-particle energies  $W(\alpha_3)$  are given by [24]

$$\begin{aligned} & (W(\alpha_3) - \varepsilon_i - W(\alpha_2)) \langle \alpha_3 | (c_i^\dagger P^+(\alpha_2))_{\alpha_3} | 0 \rangle \\ &= \sum_{j\beta_2} \left\{ \sum_k (W(\beta_2) - \varepsilon_i - \varepsilon_k) A(i\alpha_2, j\beta_2; k) \right\} \langle \alpha_3 | (c_j^\dagger P^+(\beta_2))_{\alpha_3} | 0 \rangle, \quad (9) \end{aligned}$$

where Latin letters label single-particle states and  $\varepsilon$  are the corresponding single-particle energies. The  $n$ -particle correlated states are labelled by Greek letters with the subindex  $n$ . For instance  $\alpha_3$  ( $\beta_2$ ), is a three (two) particle correlated state carrying energy  $W(\alpha_3)$  ( $W(\beta_2)$ ). The function  $A$  is

$$A(i\alpha_2, j\beta_2; k) = \hat{\alpha}_2 \hat{\beta}_2 Y(kj; \alpha_2) Y(ki; \beta_2) \begin{Bmatrix} i & k & \beta_2 \\ j & \alpha_3 & \alpha_2 \end{Bmatrix}, \quad (10)$$

and

$$Y(ij; \alpha_2) = (1 + \delta(i, j))^{1/2} X(ij; \alpha_2). \quad (11)$$

The matrix defined in Eq. (9) is not hermitian and the dimension may be larger than the corresponding shell-model dimension. This is due to the violations of the Pauli principle as well as overcounting of states in the CXMSM basis. Therefore the direct diagonalization of Eq. (9) is not convenient. One needs to calculate the overlap matrix in order to transform the CXMSM basis

into an orthonormal set. In this three-particle case the overlap matrix is

$$\langle 0|(c_i^+ P^+(\alpha_2))_{\alpha_3}^\dagger (c_j^+ P^+(\beta_2))_{\alpha_3}|0\rangle = \delta_{ij}\delta_{\alpha_2\beta_2} + \sum_k A(i\alpha_2, j\beta_2; k). \quad (12)$$

Using the overlap one can transform the matrix determined by Eq. (9) into a hermitian matrix  $T$  which has the right dimension. The diagonalization of  $T$  provides the three-particle energies. The corresponding wave function amplitudes can be readily evaluated to obtain

$$|\alpha_3\rangle = P^+(\alpha_3)|0\rangle, \quad (13)$$

$$P^+(\alpha_3) = \sum_{i\alpha_2} X(i\alpha_2; \alpha_3)(c_i^+ P^+(\alpha_2))_{\alpha_3}, \quad (14)$$

where  $P^+(\alpha_3)$  is the three-particle creation operator.

It has to be pointed out that in cases where the basis is overcomplete the amplitudes  $X$  are not uniquely defined and, therefore, they do not have physical meaning. Instead, the projection of the basis vector upon the corresponding physical vector, i.e.,

$$F(i\alpha_2; \alpha_3) = \langle \alpha_3|(c_i^+ P^+(\alpha_2))_{\alpha_3}|0\rangle, \quad (15)$$

is well defined.

That the CXMSM wave function amplitudes are usually not well defined is no hinder to evaluate the physical quantities. For details see Ref. [24]. It has to be pointed out that this feature does not appear when the basis is orthonormal, as in the one-proton three-neutron case to be analyzed below, since neither the Pauli principle nor overcounting of states are relevant here.

The next step in our CXMSM is the evaluation of the three-neutron one-proton states. With the basis denoted as

$$|p\alpha_3; \alpha_4\rangle = (c_p^+ P^+(\alpha_3))_{\alpha_4}|0\rangle, \quad (16)$$

where  $p$  labels the proton state,  $\alpha_3$  is as in Eq. (13) and  $\alpha_4$  are the three-neutron one-proton state, the four-particle energies  $W(\alpha_4)$  in  $^{12}\text{Li}$  are given by

$$\begin{aligned} & (W(\alpha_4) - \varepsilon_p - W(\alpha_3))\langle \alpha_4|(c_p^+ P^+(\alpha_3))_{\alpha_4}|0\rangle \\ &= \sum_{q\beta_3} \left\{ \sum_{kl\lambda\alpha_2} \langle pk; \lambda|V|ql; \lambda\rangle B_1 + \sum_{ijkl\lambda\alpha_2\beta_2} \langle pi; \lambda|V|ql; \lambda\rangle B_2 \right\} \\ & \times \langle \alpha_4|(c_q^+ P^+(\beta_3))_{\alpha_4}|0\rangle, \end{aligned} \quad (17)$$

where,

$$B_1 = (-1)^{p+q+k+l} X(k\alpha_2; \alpha_3) F(l\alpha_2; \beta_3) \\ \times \hat{\alpha}_3 \hat{\beta}_3 \hat{\lambda}^2 \left\{ \begin{array}{ccc} p & k & \lambda \\ \alpha_2 & \alpha_4 & \alpha_3 \end{array} \right\} \left\{ \begin{array}{ccc} q & l & \lambda \\ \alpha_2 & \alpha_4 & \beta_3 \end{array} \right\}, \quad (18)$$

and

$$B_2 = (-1)^{p+q+i+l} Y(ji; \alpha_2) Y(jk; \beta_2) X(k\alpha_2; \alpha_3) F(l\beta_2; \beta_3) \\ \times \hat{\alpha}_2 \hat{\alpha}_3 \hat{\beta}_2 \hat{\beta}_3 \hat{\lambda}^2 \left\{ \begin{array}{ccc} p & i & \lambda \\ \beta_2 & \alpha_4 & \alpha_3 \end{array} \right\} \left\{ \begin{array}{ccc} q & l & \lambda \\ \beta_2 & \alpha_4 & \beta_3 \end{array} \right\} \left\{ \begin{array}{ccc} i & j & \alpha_2 \\ k & \alpha_3 & \beta_2 \end{array} \right\}. \quad (19)$$

Here  $p$  and  $q$  label proton states, while  $i, j, k, l$  label neutron states. The proton-neutron interaction matrix elements  $\langle pk; \lambda | V | ql; \lambda \rangle$  will be discussed in the Applications. The wave function amplitudes  $X$  and the projected quantities  $F$ , defined above (Eq. (15)), have been evaluated in previous steps of the CXMSM. Notice that in this case the overlap matrix is the unit matrix, i.e.,

$$\langle 0 | (c_{p'}^+ P^+(\alpha'_3))_{\alpha_4}^\dagger (c_p^+ P^+(\alpha_3))_{\alpha_4} | 0 \rangle = \delta_{pp'} \delta_{\alpha_3 \alpha'_3} \quad (20)$$

The advantage of the MSM in stable nuclei is that one can study the influence of collective vibrations upon nuclear spectra within the framework of the shell model. Thus, in Ref. [24] the multiple structure of particle-vibration coupled states in odd Pb isotopes was analyzed. But the most important feature for our purpose is that the CXMSM allows one to choose in the basis states a limited number of excitations. This is because in the continuum the vast majority of basis states consists of scattering functions. These do not affect greatly physically meaningful two-particle states. That is, the majority of the two-particle states provided by the CXSM are complex states which form a part of the continuum background. Only a few of those calculated states are relevant, namely the ones that are mainly built upon poles. The question of how to evaluate and recognize the physically meaningful three-particle states, are addressed in the next Section.

### 3. Applications

In this Section we will apply the CXMSM formalism described above to study the nucleus  $^{12}\text{Li}$ .

To evaluate the valence shells we will proceed as in Refs. [19, 22, 25] and choose as central field a Woods-Saxon potential with different depths for even and odd orbital angular momenta  $l$ . The corresponding parameters are (in parenthesis for odd  $l$ -values)  $a= 0.670$  fm,  $r_0 = 1.27$  fm,  $V_0 = 50.0$  (36.9) MeV and  $V_{\text{so}}=16.5$  (12.6) MeV. As in Ref. [19], we thus found the single-particle bound states  $0s_{1/2}$  at -23.280 MeV and  $0p_{3/2}$  at -2.589 MeV. The valence shells are the low lying resonances  $0p_{1/2}$  at (0.195,-0.047) MeV and  $0d_{5/2}$  at (2.731, -0.545) MeV and the shell  $0d_{3/2}$  at (6.458,-5.003) MeV. This cannot be considered a resonance, since it is so wide that rather it is a part of the continuum background. Besides, the state  $1s_{1/2}$  appears as an antibound state at -0.050 MeV. We thus reproduce the experimental single-particle energies as given in Ref. [26]. We also found other states at higher energies, but they do not affect our calculation because they are very high and also very wide. We thus include in our Berggren representation only the antibound state  $1s_{1/2}$  and the resonances  $0p_{1/2}$  and  $0d_{5/2}$ .

To define the Berggren single-particle representation we still have to choose the integration contour  $L^+$  (see Eq. (1)).

To include in the representation the antibound  $1s_{1/2}$  state as well as the Gamow resonances  $0p_{1/2}$  and  $0d_{5/2}$  we will use two different contours. The number of points on each contour define the energies of the scattering functions in the Berggren representation, i.e., the number of basis states corresponding to the continuum background. This number is not uniformly distributed, since in segments of the contour which are close to the antibound state or to a resonance the scattering functions increase strongly. We therefore chose the density of points to be larger in those segments.

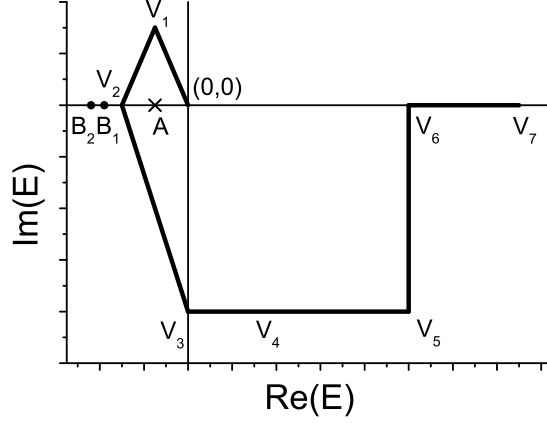


Figure 1: Contour used to include the antibound state (see, also, Ref. [19]). The points  $B_i$  denote bound states while  $A$  denotes the antibound state. The points  $V_i$  correspond to the vertices defining the contour. They have the values  $V_1=(-0.05,0.05)$  MeV,  $V_2=(-0.1,0)$  MeV,  $V_3=(0,-0.4)$  MeV,  $V_4=(0.5,-0.4)$  MeV,  $V_5=(8,-0.4)$  MeV,  $V_6=(8,0)$  MeV and  $V_7=(10,0)$  MeV

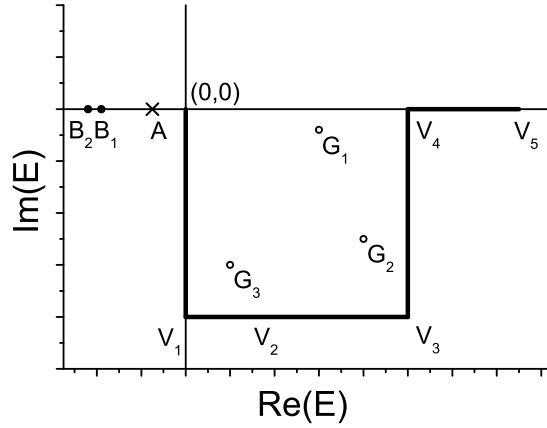


Figure 2: Contour used to include the Gamow resonances represented by the points  $G_i$ . The vertices are  $V_1=(0,-1)$  MeV,  $V_2=(1,-1)$  MeV,  $V_3=(8,-1)$  MeV,  $V_4=(8,0)$  MeV and  $V_5=(10,0)$  MeV.

Table 1: Number of Gaussian points in the different segments of the contour of Fig. 1.

| Segment | $[(0, 0) - V_1]$ | $[V_1 - V_2]$ | $[V_2 - V_3]$ | $[V_3 - V_4]$ | $[V_4 - V_5]$ | $[V_5 - V_6]$ | $[V_6 - V_7]$ |
|---------|------------------|---------------|---------------|---------------|---------------|---------------|---------------|
| Number  | 30               | 30            | 30            | 30            | 30            | 16            | 6             |

Table 2: Number of Gaussian points in the different segments of the contour of Fig. 2.

| Segment | $[(0, 0) - V_1]$ | $[V_1 - V_2]$ | $[V_2 - V_3]$ | $[V_3 - V_4]$ | $[V_4 - V_5]$ |
|---------|------------------|---------------|---------------|---------------|---------------|
| Number  | 30               | 30            | 30            | 8             | 4             |

We include the antibound state by using the contour in Fig. 1. The number of points in each segment are given in Table 1. For the Gamow resonances the contour in Fig. 2 is used with the number of Gaussian points as in Table 2.

We have adopted these points after verifying that the results converged to their final values. A discussion about the choice of these contours and also on the physical meaning of the antibound state can be found in Ref. [20].

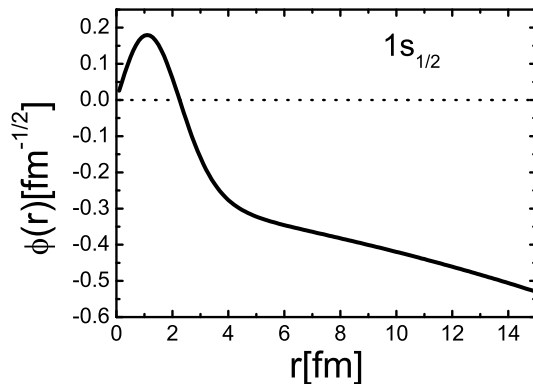


Figure 3: Radial function  $\phi(r)$  corresponding to the single-particle neutron antibound state  $0s_{1/2}$  at an energy of  $-0.050$  MeV.

To explore the extend to which the poles are physically meaningful we plotted in Fig. 3 the  $1s_{1/2}$  antibound state. One sees that it extends in an increasing rate far out from the nuclear surface, as expected in this halo nucleus (the standard value of the radius is here  $1.2 \times 11^{1/3} = 2.7$  fm). The radial wave function corresponding to the Gamow resonance  $0p_{1/2}$  is shown in Fig. 4. The resonance  $0d_{5/2}$  has a large and increasing imaginary part at relative short distances, as shown in Fig. 5.

With the single-particle representation thus defined we proceed to evaluate the two-particle states.

### 3.1. Two-particle states: the nucleus $^{11}\text{Li}$ .

We would like to start this Subsection by stressing, once again, that the two-particle states that we will investigate here correspond to two-neutron excitations in the spectrum of  $^{11}\text{Li}$ , while the corresponding odd proton is

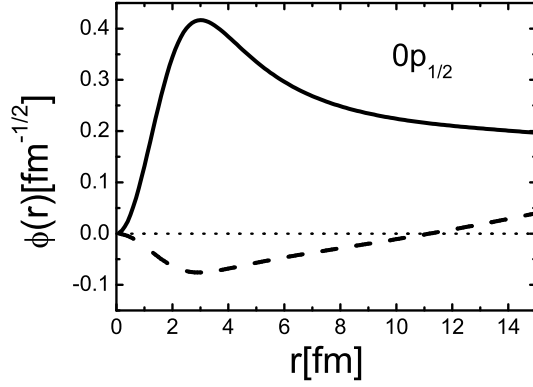


Figure 4: As Fig. 3 for the Gamow resonance  $0p_{1/2}$  at an energy of (0.195,-0.047) MeV. The dashed line is the imaginary part of the wave function.

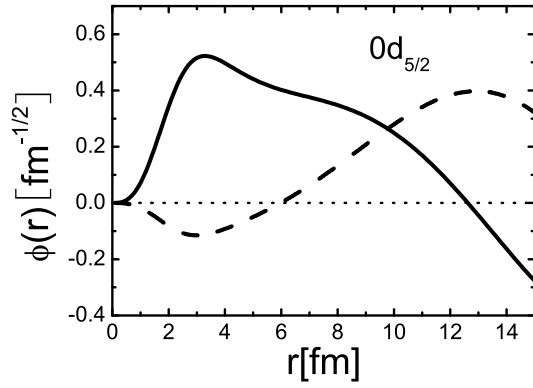


Figure 5: As Fig. 3 for the Gamow resonance  $0d_{5/2}$  at an energy of (2.731,-0.545) MeV. The dashed line is the imaginary part of the wave function.

an spectator. To avoid confusions in what follows we will call these states  $^{11}\text{Li}(2\nu; J)$ , where  $2\nu$  indicates that the state  $J$ , which belongs to the spectrum of  $^{11}\text{Li}$ , is determined by two-neutron excitations.

The only state which is measured in  $^{11}\text{Li}$  is its bound ground state, which was found to lie at an energy of -0.369 MeV [27]. The corresponding angular momentum is  $3/2^-$ . This spin arises from the odd inert proton, lying deep in the spectrum, coupled to two neutrons. The dynamics of the system is thus determined by the pairing force acting upon the two neutrons coupled to a state  $0^+$ , which behaves as a normal even-even ground state [20, 22]. Besides the energy, this state has been measured to have an angular momentum contain of about 60% of s-waves and 40% of p-waves, although small components of other angular momenta are not excluded [21].

We will perform the calculation of the two-particle states by using the separable interaction discussed in Section 2. The strength  $G_{\lambda_2}$ , corresponding to the states with angular momentum  $\lambda_2$  and parity  $(-1)^{\lambda_2}$ , will be determined by fitting the experimental energy of the lowest of these states, as usual. It is worthwhile to point out that  $G_{\lambda_2}$  defines the Hamiltonian and, therefore, is a real quantity. The two-particle energies are found by solving the corresponding dispersion relation while the two-particle wave function components are as in Eq. (8).

With the quantities entering the two-particle TDA equations thus determined we evaluated the two-neutron states in  $^{11}\text{Li}(2\nu; J = 0^+)$ . We found that the angular momentum contain of the ground state wave function is 46.8% *s*-states, 49.1% *p*-states and 4.2% *d*-states. This is in reasonable agreement with experiment [21].

The wave function components corresponding to  $^{11}\text{Li}(2\nu; gs)$  are strongly dependent upon the contour that one uses. However, measurable quantities, like the energies and transition probabilities, do not. This is because the physical quantities are defined on the real energy axis and, therefore, they remain the same when changing contour. But complex states which are part of the continuum background do not have any counterpart on the real energy axis and the physical quantities for these states acquire different values for different contours [20]. We will use this property to determine whether a complex state is a meaningful resonance. This is important, since the ground state is the only one for which experimental data exists. There might be other meaningful states that have not been found yet. This implies that we have to evaluate all possible two-particle states which are spanned by our single-particle representation. For the purpose of this paper this is an important

task, since in the next step of the CXMSM only physically meaningful states will be considered as members of the basis.

To decide whether a calculated state is a meaningful resonance we will proceed as in Refs. [20, 28] and analyze the singlet ( $S=0$ ) component of the two-particle wave function. The corresponding expression for this component was given in Eq. (10) of Ref. [28], but we will show it here again for clarity of presentation. For the state  $\alpha$  with spin and spin-projection ( $JM$ ) that component is, with standard notation,

$$\begin{aligned} \Psi_{\alpha JM}(\vec{r}_1 \vec{r}_2) = & [\chi_{1/2}(1)\chi_{1/2}(2)]_0^0 \sum_{a \leq b} X(ab, \alpha JM) \hat{j}_a \hat{j}_b \\ & \times [C(ab, \vec{r}_1 \vec{r}_2) - (-)^{j_a + j_b - J} C(ba, \vec{r}_1 \vec{r}_2)], \quad (21) \end{aligned}$$

where

$$C(ab, \vec{r}_1 \vec{r}_2) = \phi_a(r_1)\phi_b(r_2)(-)^{l_b + 1/2 - j_a + J} \left\{ \begin{matrix} l_a & j_a & 1/2 \\ j_b & l_b & J \end{matrix} \right\} [Y_{l_a}(\hat{r}_1)Y_{l_b}(\hat{r}_2)]_{JM}, \quad (22)$$

and  $\phi_a(r)$  is the radial wave function corresponding to the single-particle state  $a$  (Eq. (3)).

If the two-particle state ( $\alpha JM$ ) is a meaningful resonance then the wave function above should be localized within a region extending not too far outside the nuclear surface, and its imaginary part should not be too large [20]. To study these features it is not necessary to go to all six dimensions corresponding to the coordinates  $\vec{r}_1$  and  $\vec{r}_2$ . In fact it is enough to consider the coordinate  $r$  given by  $\vec{r}_1 = \vec{r}_2 = \vec{r} = (0, 0, r)$  which corresponds to the two particles located at the same point and in the z-direction. For details see [28]. We will call this one-dimensional function  $\Psi_{\alpha JM}(r)$ .

The evaluation of the  $0^+$  states is a relatively easy task, since in this case we have determined the strength  $G_{0^+}$  by fitting the experimental energy of  $^{11}\text{Li}(2\nu; gs)$ . With this value of the strength we calculated all the  $0^+$  states and found that the vast majority of them are continuum states which belong to the background. The relevant states are those which are built mainly from the poles [8, 9]. Although these states may not be in themselves physically meaningful resonances, they can influence significantly the spectrum of  $^{12}\text{Li}$ .

We therefore included in the CXMSM basis those two-particle states which have at least one pole configuration which, in absolute value, is 0.3 or larger. We found that all these states correspond to the poles  $1s_{1/2}$  and  $0p_{1/2}$

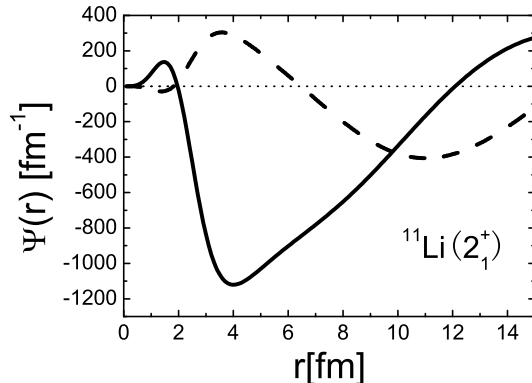


Figure 6: Radial function  $\Psi(r)$  corresponding to the two-particle state  $^{11}\text{Li}(2\nu; 2_1^+)$  at an energy of (2.300,-0.372)MeV. The dashed line is the imaginary part of the wave function.

coupled to themselves or to continuum states lying close to threshold. As a result, these are narrow states. We found also similar meaningful  $1^-$  and  $2^+$  states. Specially important is the state  $1^-$  at (0.084,-0.002) MeV which is built by the pole configuration  $(0s_{1/2}0p_{1/2})_{1^-}$  and therefore may be physically meaningful. Also the state  $2_1^+$  at (2.300,-0.372) MeV which is practically built by the pole configuration  $(0s_{1/2}0d_{5/2})_{2^+}$  can be meaningful. However its width (i. e. 0.744 MeV) seems to be too large and therefore we decided to analyze the corresponding radial wave function in more detail. For this we drew  $\Psi_{2_1^+}(r)$ , as shown in Fig. 6. One sees that the wave function is rather localized and that its imaginary part is relatively small as compared to the corresponding real part. This is a state which perhaps is at the limit of what can be considered a meaningful resonance. Yet, it has an effect on the physical three-particle states, as will be seen below. It is worthwhile to point out that the width of this state (744 keV) is the escape width. At high energies, where the giant resonances lie, most of the width consists of the spreading width, i.e., of mixing with particle-hole configurations [29]. However, at the low energies of the states that we study this mixing is not relevant.

An important point for the analysis of the three-particle states to be performed below, is that the scattering wave functions in the segments  $[(0, 0) - V_1]$ ,  $[V_1 - V_2]$  and  $[V_2 - V_3]$  are similar in magnitude to the wave function of the antibound state. This is because the segments are very close to the antibound state [20]. This is a feature that cannot be avoided, and is due

to the attractive character of the pairing force. That is, the lowest single-particle configuration in the Berggren basis is  $V_2^2$ , with energy  $-2\epsilon$ , where  $V_2 = (-\epsilon, 0)$ . This configuration has to lie *above* the energy of the two-particle correlated state, i.e., it has to be  $\epsilon > \omega(^{11}\text{Li}(2\nu; gs))/2$ .

With the states  $0^+$ ,  $1^-$  and  $2^+$  thus calculated we proceeded to the calculation of the three-particle system within the CXMSM.

### 3.2. Three-particle states

Using the single- and two-particle neutron states discussed above, we formed all the possible three-particle basis states. Due to the large number of scattering states included in the single-particle representation the dimension of the three-particle basis is also large. The scattering states are needed in order to describe these unstable states.

With the CXMSM basis thus constructed we evaluated the dynamical matrix Eq. (9) and the overlap Eq. (12). With these we formed the symmetric Hamiltonian matrix which we diagonalized to obtain the three-neutron states. We found that the lowest state is  $1/2^+$  at  $(-0.381, +0.023)$  MeV. That is, the energy is real and negative. It is an antibound state, as it is the  $1s_{1/2}$  state itself. A manifestation of this is that the radial wave function diverges at large distances.

With the three-neutron states thus calculated and the proton state  $0p_{3/2}$  we constructed the final CXMSM basis to describe the nucleus  $^{12}\text{Li}$ .

### 3.3. Four-particle states

In this case the one-proton three-neutron CXMSM basis is orthonormal and the matrix (17) is already the Hamiltonian matrix. All the three-neutron quantities appearing in Eq. (17) have been solved in the previous step of the CXMSM. Instead, the single-proton energy and the proton-neutron interaction matrix elements are quantities that we have still to determine. The single-proton energy was not considered so far. When we evaluated the ground state of  $^{11}\text{Li}(2\nu)$  we assumed that its energy was only determined by the two-neutron excitations. The value of the energy was obtained by fitting the strength of the neutron-neutron separable interaction, ignoring any effect that the protons may have had. In the analysis of the spectrum of  $^{11}\text{Li}$ , including the wave functions, this is irrelevant, since the assumption in those calculations was that the protons were only spectators. In other words, the effect of the odd proton was only an scaling of the energies. A similar feature occurs in the evaluation of the three-neutron one-proton states. As seen in

Eq. (17) the value of the proton energy  $\varepsilon_p$ , where  $p$  is the proton state  $0p_{3/2}$ , only shift the spectrum, but the relative energy between two given states is not affected. Again here the effect of the proton degree of freedom regarding the single-particle energy is to scale the whole spectrum of  $^{12}\text{Li}$ .

The determination of  $\varepsilon_p$  is a difficult task due to the energy renormalizations that our procedure implies. However, it should be a real number, since the proton is a bound state. We will, therefore, not intend to evaluate the absolute energies and only discuss the  $^{12}\text{Li}$  energies relative to the corresponding ground state energy. This is equivalent to take  $\varepsilon_p$  as a real parameter that adjust the real part of the ground state energy of  $^{12}\text{Li}$ . The proton-neutron interaction matrix elements were taken from empirical effective interactions which are determined by fitting experimental data [30, 31].

With the quantities entering the Hamiltonian matrix (17) determined as discussed above, we calculated the energies  $W(\alpha_4)$  and the wave function amplitudes  $\langle \alpha_4 | (c_p^+ P^+(\alpha_3))_{\alpha_4} | 0 \rangle$ . Notice that in this case of an orthonormal basis the wave function components  $X$  and the corresponding projections  $F$  (Eq. (15)) coincide.

Due to the presence of the continuum states the dimension of the one-proton three-neutron basis is very large. Of all the states calculated within this basis we will present only those which are physically meaningful. As we have discussed above, the main configurations in such states contain large contributions from the poles (relevant configurations). We therefore will proceed as in the evaluation of the two-neutron states and consider physically meaningful the one-proton three-neutron basis states for which at least the amplitude of one relevant configuration is, in absolute value, 0.3 or larger.

Below we will briefly describe the structure of the states thus calculated forming the  $^{12}\text{Li}$  spectrum.

As seen in Fig. 7 there are five states at low energy predicted by the theory. All of them are narrow and mainly built upon configurations that are close to the continuum threshold. This is not surprising since the determining poles at low energy are the antibound state  $s_{1/2}$  and the resonance  $p_{1/2}$ , and both have real or nearly real energies and are very close to threshold..

The  $^{12}\text{Li}$  ground state is  $2^-$  and its energy is real. Since it is neither a bound state (its wave function diverges at large distances) neither a resonance (its energy is a real quantity) we conclude that it is an antibound state. This is not surprising, since it is mainly built upon the CXMSM basis state  $|\pi(0p_{3/2})\nu(1s_{1/2} \otimes^{11}\text{Li}(2\nu; \text{gs}))_{1/2^+} 2^-\rangle$ , where  $\pi$  ( $\nu$ ) indicates proton (neutron) degree of freedom. The three-neutron component of this state is

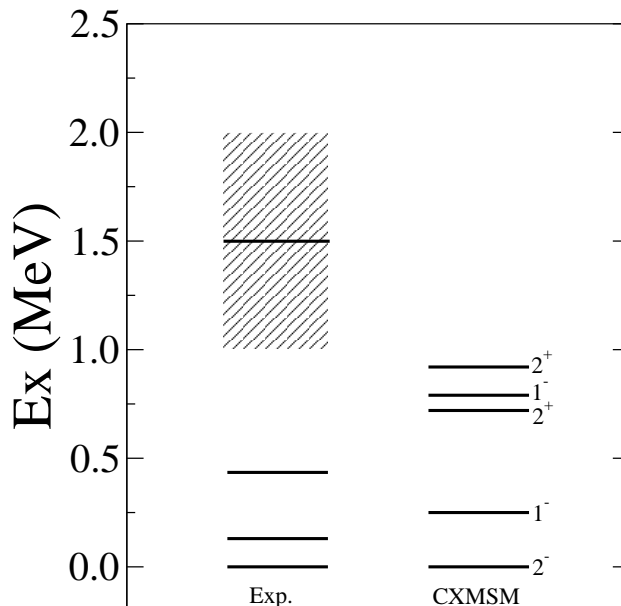


Figure 7: Experimental level scheme in  $^{12}\text{Li}$ . The three lowest levels are from [7], while the one at 1.5 MeV is from [6]. The theoretical results are labelled CXMSM.

dominated by the state  $\nu(1s_{1/2})$  and this induces the state  $2_1^-$  to be antibound. It is worthwhile to point out that the influence of the  $\nu(1s_{1/2})$  antibound single-particle state is due to its position, lying very close to the continuum threshold. Since there is no barrier to trap inside the nucleus the neutron moving in this state, the corresponding wave function is very similar to the one corresponding to a bound state at the same small and negative energy [20]. Within the Continuum Shell Model the influence of the antibound state is taken into account by the scattering states on the real energy axis lying close to the continuum threshold [32]. Even in the complex energy plane the scattering wave functions lying close to the antibound state are similar to each other [20, 33]. A discussion on the conveniences and drawbacks of using the complex energy plane to describe the antibound state can be found in Ref. [33].

The question one may ask is how is it possible that in  $^{12}\text{Li}$  three neutrons can occupy the state  $1s_{1/2}$ . The answer to this is that in the continuum this state is split in many components.

The other states at low energy in Fig. 7 are built upon the proton single-particle state  $0p_{3/2}$  coupled to the three-neutron states  $|1s_{1/2} \otimes ^{11}\text{Li}(2\nu; 0^+)\rangle$ ,

$|1s_{1/2} \otimes^{11}\text{Li}(2\nu; 1^-)\rangle$ ,  $|0p_{1/2} \otimes^{11}\text{Li}(2\nu; 0^+)\rangle$  and  $|0p_{1/2} \otimes^{11}\text{Li}(2\nu; 1^-)\rangle$ . They are all narrow states.

Besides these states there are many levels that lie above 1 MeV which are built upon the pole  $0d_{5/2}$ . This may explain the broad resonance seen experimentally at about 1.5 MeV.

The experiment shows two narrow excited states below 0.5 MeV, which the calculation predicts to be  $1^-$  and  $2^+$ , respectively.

Most of the calculated levels in Fig. 7 are strongly influenced by the continuum states. If we would take only relevant configurations with amplitudes larger than 0.9 then only two states would appear. If no continuum configurations are included then no excited state below 1.1 MeV would be found, as can be seen in the shell model calculation of Ref. [7].

#### 4. Summary and conclusions

In this paper we have studied excitations occurring in the continuum part of the nuclear spectrum which are at the limit of what can be observed within present experimental facilities. These states are very unstable but yet live a time long enough to be amenable to be treated within stationary formalisms. We have thus adopted the CXSM (shell model in the complex energy plane [12]) for this purpose. In addition we performed the shell model calculation by using the multistep shell model. In this method of solving the shell model equations one proceeds in several steps. In each step one constructs building blocks to be used in future steps [10]. We applied this formalism to analyze the spectrum of  $^{12}\text{Li}$  by assuming that it is determined by one-proton three-neutron excitations. First we studied the neutron degrees of freedom by profiting from the information that exists on the single-neutron states in  $^{10}\text{Li}$  and on two-neutron states in  $^{11}\text{Li}$ . In our case of  $^{12}\text{Li}$  the neutron excitations correspond to the motion of three neutrons, partitioned as the one- times two-neutron systems. This formalism was applied before, e.g., to study multiplets in the lead region [24]. Finally, the spectrum of  $^{12}\text{Li}$  is calculated by coupling the three-neutron system with the  $0p_{3/2}$  single-proton state.

We adopted the single-particle energies (i.e., states in  $^{10}\text{Li}$ ) as provided by experimental data when available or as provided by our calculation. These are the antibound state  $1s_{1/2}$  and the resonances  $0p_{1/2}$  and  $0d_{5/2}$ . Besides these states (which are poles of the Green function) we also included continuum states (Coulomb waves). We found that the physically meaningful two-neutron states are mainly built upon poles. With the two-particle states

thus obtained we calculated the three-neutron states and coupled them to the  $0p_{3/2}$  protons state to evaluate the spectrum of  $^{12}\text{Li}$ . The ground state energy of this nucleus turns out to be real. Since this is neither a bound state (the wave function diverge at large distances) nor a resonance (the energy is real) we conclude that it is an antibound state. This agrees with a number of experiments [5, 6, 7].

Besides this antibound state our calculation predicts two low lying narrow states which, as seen in Fig. 7, are also found experimentally. But there are also three other calculated levels which have not been observed so far.

We conclude that the experimentally observed narrow states in  $^{12}\text{Li}$  arise as a result of the valence neutrons moving in unstable shells. As in  $^{11}\text{Li}$ , these are mainly the antibound state  $1s_{1/2}$  and the narrow resonance  $0p_{1/2}$ . But in  $^{12}\text{Li}$  continuum states lying close to threshold play also a fundamental role.

## 5. Acknowledgments

This work has been supported by the Swedish Research Council (VR). Z.X. is supported in part by the China Scholarship Council under grant No. 2008601032.

## References

- [1] V. Rotival, K. Bennaceur, T. Duguet, Phys. Rev. C 79 (2009) 054309.
- [2] N. Schunck, J.L. Egido, Phys. Rev. C 78 (2008) 064305.
- [3] M. Grasso, S. Yoshida, N. Sandulescu, N. V. Giai, Phys. Rev. C 74 (2006) 064317.
- [4] T. Baumann et al., Nature 449 (2007) 1022.
- [5] Yu. Aksyutina et al., Phys. Lett. B 666 (2008) 430.
- [6] T. Roger, PhD thesis; P. Roussel Chomaz et al., to be published.
- [7] C. C. Hall et al., Phys. Rev. C 81 (2010) 021302(R).
- [8] R. Id Betan, R. J. Liotta, N. Sandulescu, T. Vertse, Phys. Rev. Lett. 89 (2002) 042051.

- [9] N. Michel, W. Nazarewicz, M. Płoszajczak, K. Bennaceur, Phys. Rev. Lett. 89 (2002) 042502.
- [10] R. J. Liotta, C. Pomar, Phys. A 382 (1982) 1.
- [11] G. Gamow, Z. Phys. 51 (1928) 204.
- [12] R. Id Betan, R. J. Liotta, N. Sandulescu, T. Vertse, Phys. Rev. C 67 (2003) 014322.
- [13] N. Michel, W. Nazarewicz, M. Płoszajczak, T. Vertse, J. Phys. G 36 (2009) 013101.
- [14] T. Berggren, Nucl. Phys. A 109 (1968) 265.
- [15] I. J. Thompson, M. V. Zhukov, Phys. Rev. C 49 (1994) 1904.
- [16] R. J. Liotta, E. Maglione, N. Sandulescu, T. Vertse, Phys. Lett. B 367 (1996) 1.
- [17] N. Michel, W. Nazarewicz, M. Płoszajczak, Phys. Rev. C 70 (2004) 064313.
- [18] G. F. Bertsch, H. Esbensen, Ann. Phys. (New York) 209 (1991) 327.
- [19] R. Id Betan, R.J. Liotta, N. Sandulescu, T. Vertse, Phys. Lett. B 584 (2004) 48.
- [20] R. Id Betan, R. J. Liotta, N. Sandulescu, T. Vertse, R. Wyss, Phys. Rev. C 72 (2005) 054322.
- [21] E. Garrido, D. V. Fedorov, A. S. Jensen, Nucl. Phys. A 700 (2002) 117.
- [22] H. Esbensen, G.F. Bertsch, K. Hencken, Phys. Rev. C 56 (1997) 3054, and references therein.
- [23] N.B. Shulgina, B. Jonson, M.V. Zhukov, Nucl. Phys. A 825 (2009) 175.
- [24] J. Blomqvist, R. J. Liotta, L. Rydstrom, C. Pomar, Nucl. Phys. A 423 (1984) 253.
- [25] J.C. Pacheco, N. Vinh Mau, Phys. Rev. C 65 (2002) 044004.

- [26] H.G. Bohlen et al., Nucl. Phys. A 616 (1997) 254c.
- [27] M. Smith et al., Phys. Rev. Lett. 101 (2008) 202501.
- [28] G. G. Dussel, R. Id Betan, R. J. Liotta, T. Vertse, Phys. Rev. C 80 (2009) 064311.
- [29] S. Gales, Ch. Stoyanov, A. I. Vdovin, Phys. Rep. 166 (1988) 127.
- [30] E. K. Warburton, B. A. Brown, Phys. Rev. C 46 (1992) 923.
- [31] S. Cohen, D. Kurath, Nucl. Phys. 73 (1965) 1.
- [32] G.F. Bertsch, K. Hencken, H. Esbensen, Phys. Rev. C 57 (1998) 1366.
- [33] N. Michel, W. Nazarewicz, M. Ploszajczak, J. Rotureau, Phys. Rev. C 74 (2006) 054305.